

Supporting Information

One-step fabrication of robust and anti-oil fouling aliphatic polyketone composite membranes for sustainable and efficient filtration of oil-in-water emulsions

Lei Zhang, Liang Cheng*, Haochen Wu, Tomohisa Yoshioka, and Hideto Matsuyama*

Center for Membrane and Film Technology, Department of Chemical Science and Engineering, Kobe University, Kobe 657-8501, Japan

* Corresponding authors

E-mail: chengl@lion.kobe-u.ac.jp (L. Cheng)
matuyama@kobe-u.ac.jp (H. Matsuyama)

This file contains 9 pages, including 9 figures and 1 table.

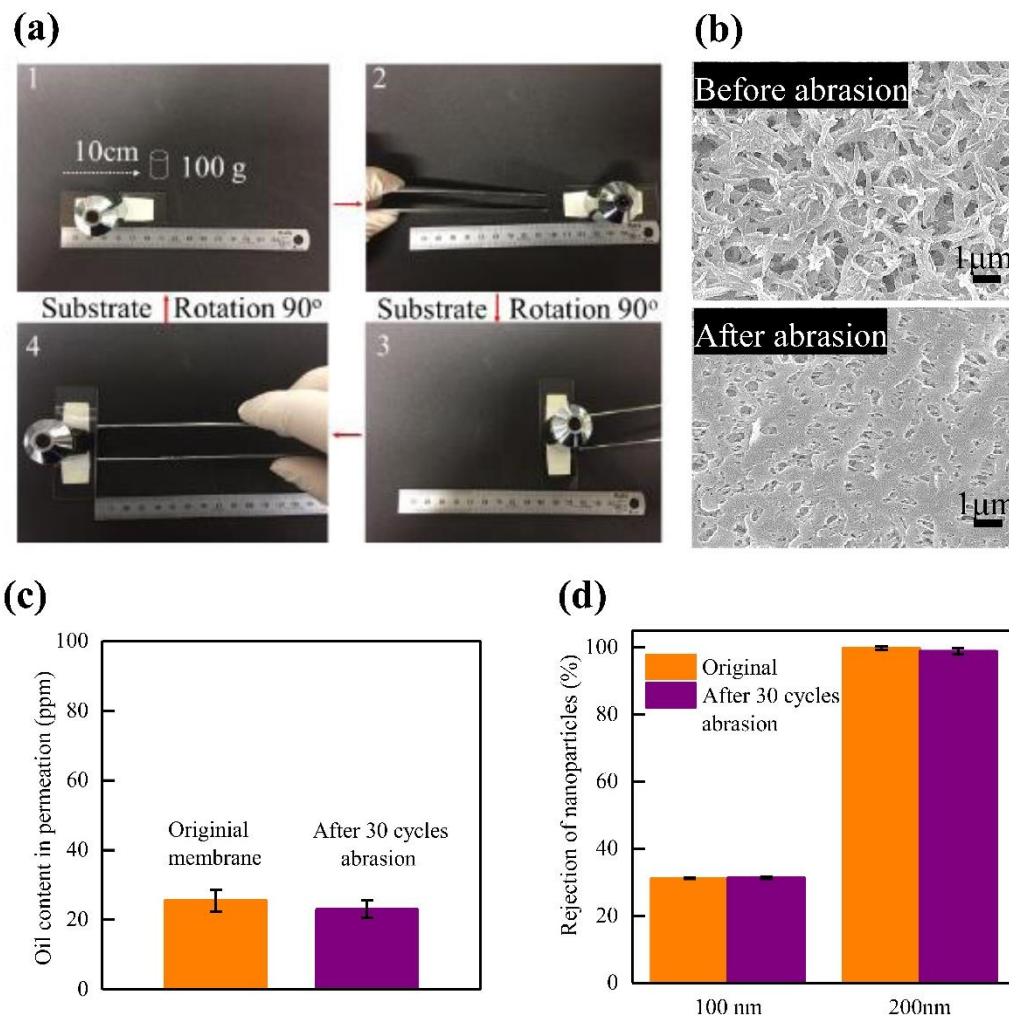


Fig. S1 Effect of abrasion test on the performances of the PK/PVA1500-Nyl composite membrane. (a) Photographs of the sandpaper abrasion test procedures including four steps in one cycle. (b) SEM images of the composite membrane surface before and after the abrasion test. (c) Oil/water separation performances before and after abrasion for the filtration of hexadecane-in-water emulsion (10000 ppm oil and 1 ppm SDS). (d) Rejections of nanoparticles before and after abrasion.

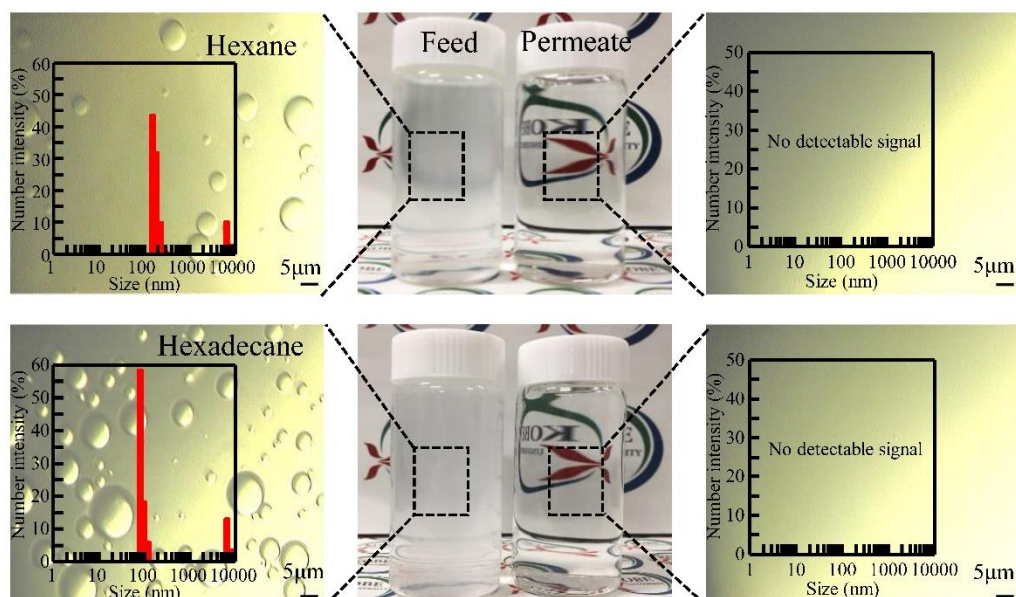


Fig. S2 Optical microscope images and digital photos of the hexane-in-water and hexadecane-in-water emulsions (10000 ppm oil and 1 ppm SDS) before and after the cross-flow membrane filtration by PK/PVA1500-Nyl under 0.1 bar. The insets shows the droplet sizes and size distribution measured by dynamic light scattering (DLS) measurements. The oil content in the permeate as analyzed by TOC was found to be 23.2 ± 2.9 and 25.5 ± 3.2 ppm for hexane-in-water and hexadecane-in-water emulsions, respectively.

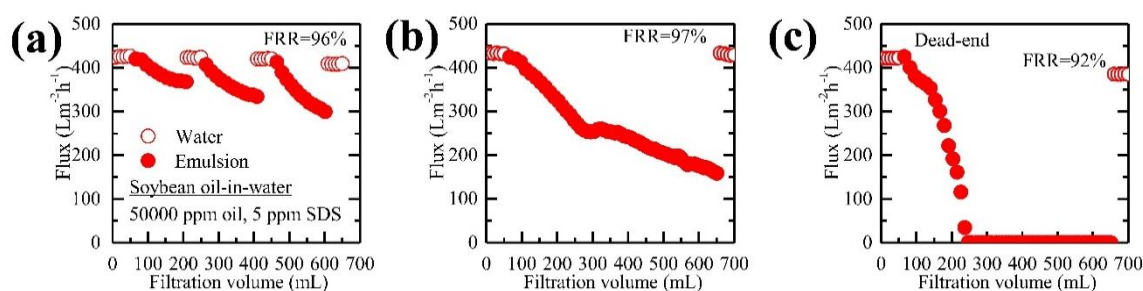


Fig. S3 Flux variations and flux recoveries after water cleaning for the filtrations of a soybean oil-in-water emulsion containing 50000 ppm oil and 5 ppm SDS by PK/PVA1500-Nyl in the cross-flow cell with (a) three times regular water cleaning, (b) only once water cleaning and (c) no circulation, equivalent to the dead-end mode.

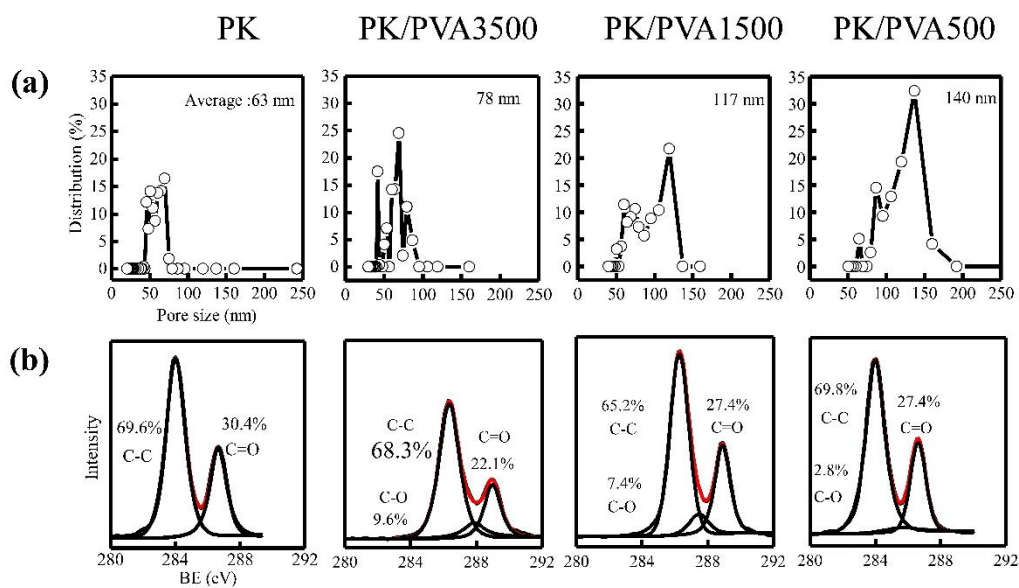


Fig. S4 Characterizations of average pore sizes and chemical compositions of the PK/PVA blend membranes.

(a) Average pore sizes analyzed using capillary flow porometer. (b) XPS C1s core-level signal.

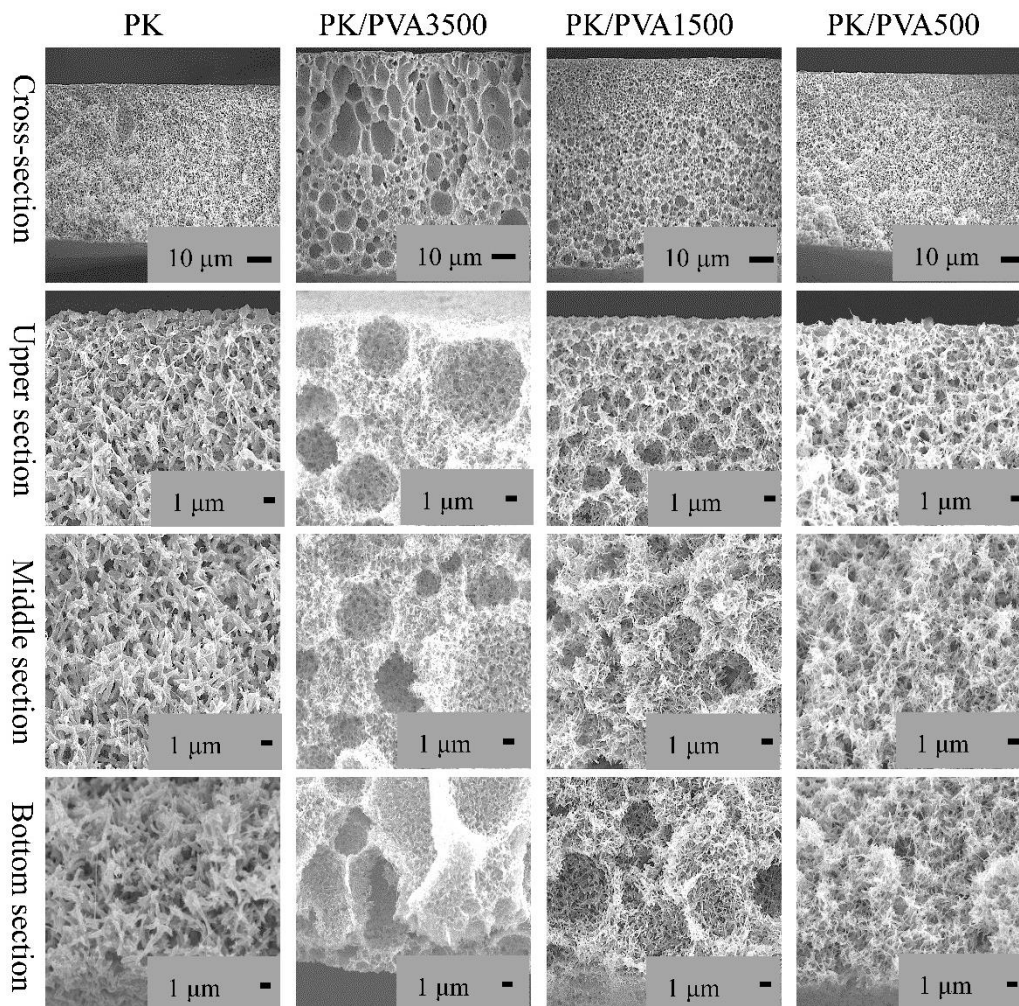


Fig. S5 Cross-section morphologies of the pure PK membrane and PK/PVA blend membranes.

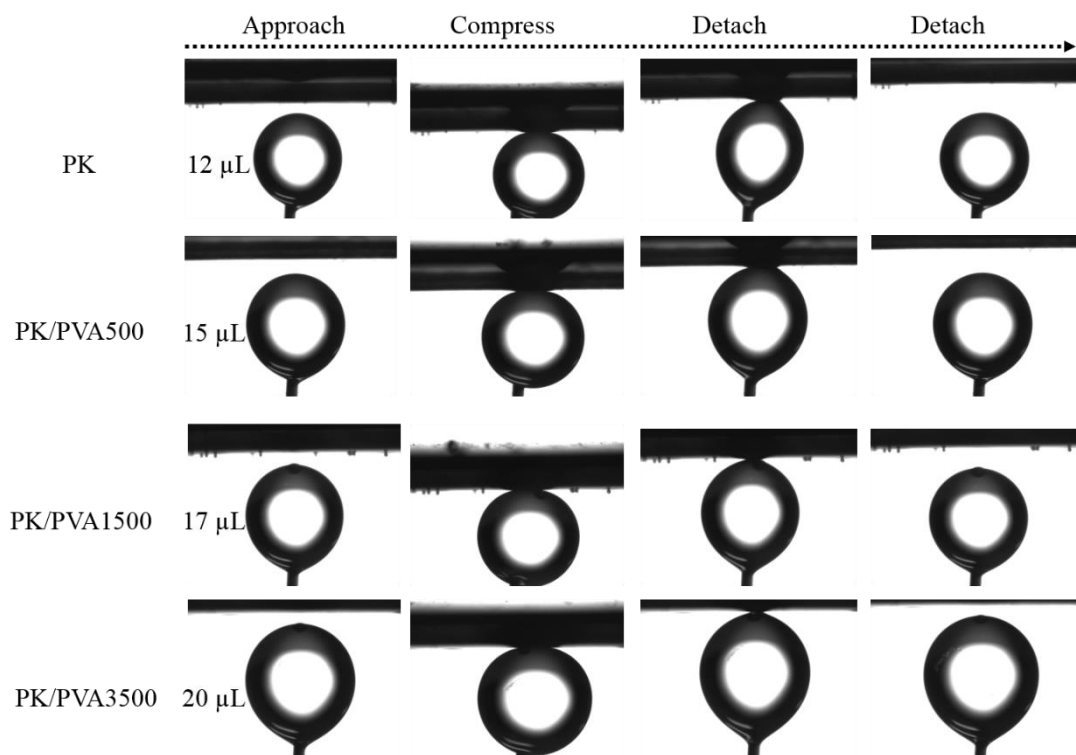


Fig. S6 Dynamic underwater soybean oil-adhesion measurements on the pure PK membrane and the PK/PVA blend membranes, showing the critical oil droplet volume beyond which the oil droplet release from the dispensing needle can be achieved.

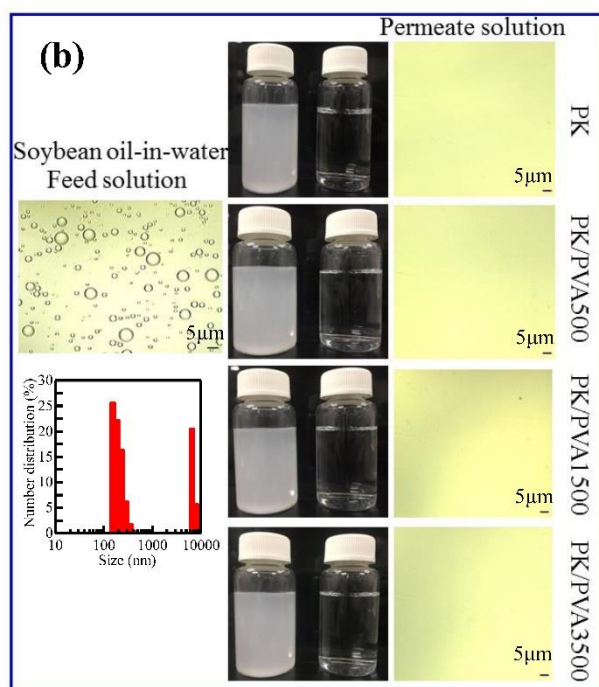
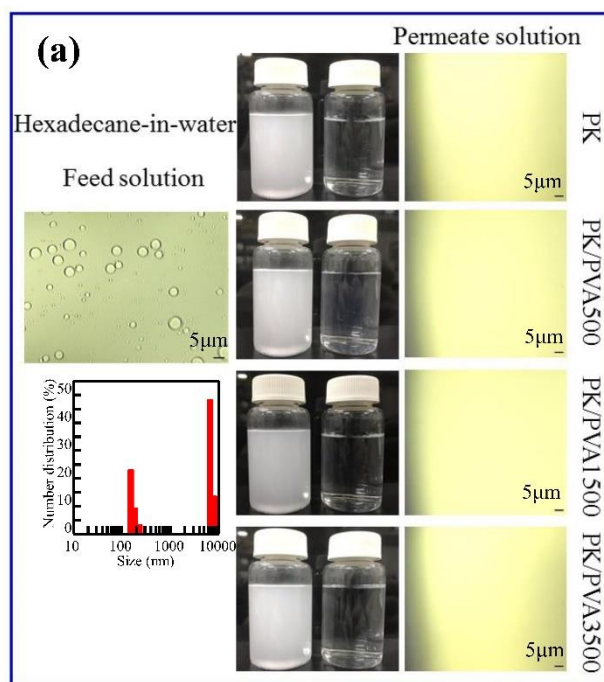


Fig. S7 Optical microscope images and digital photos of the oil-in-water emulsions (10000 ppm oil and 1 ppm SDS) before and after filtration by the PK/PVA blend membranes under the dead-end mode: (a) hexadecane-in-water emulsion and (b) soybean oil-in-water emulsion.

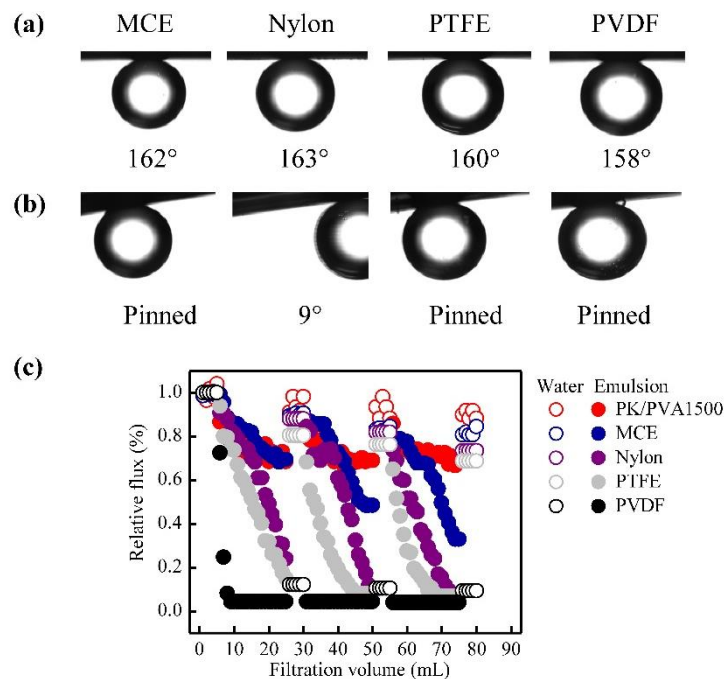


Fig. S8 Comparison of the surface wettabilities and oil-in-water emulsion filtration performances of four commercial hydrophilic membranes and PK/PVA1500: (a) underwater soybean oil contact angles; (b) underwater soybean oil sliding angles; (c) Flux variations and recoveries recorded during the filtrations of soybean oil-in-water emulsion (10000 ppm oil and 1 ppm SDS) at the same initial flux of $\sim 170 \text{ Lm}^{-2}\text{h}^{-1}$.

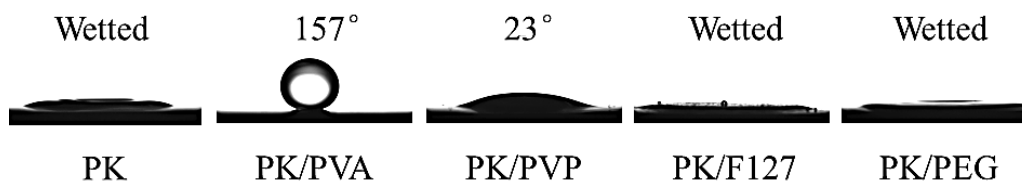


Fig. S9 Underwater chloroform contact angles on the prepared PK, PK/PVA, PK/PVP, PK/F127, and PK/PEG membranes.

Table S1 Summary of the performances of the commercial hydrophilic membranes and PK/PVA1500

Membranes	Water contact angle (°)	Underwater oil contact angle ^a (°)	Sliding angle ^a (°)	Emulsion flux ^b (Lm ⁻² h ⁻¹ 0.01 bar)	Oil rejection ^b (%)	Flux recovery ^b (%)
MCE	38	162	pinned	100	99.8	83
Nylon	43	163	9	51	99.5	74
PTFE	49	160	pinned	116	99.5	70
PVDF	62	158	pinned	21	99.6	10
PK/PVA1500	42	170	4	140	99.7	90

^aSoybean oil as the probe oil, ^bSoybean oil-in-water emulsion (10000 ppm oil and 1 ppm SDS) filtrated under gravity-driven dead-end mode under 0.01 bar.